3-Coherent Beams Phase Doppler and Laser Doppler Velocimetry Measurements Techniques

By

F. Onofri[(1)] and S. Radev[(2)]

[(1)]IUSTI- UMR n°6595 CNRS - Université de Provence

Technopôle de Château-Gombert, 13453 Marseille Cedex 13 (France)

Fabrice.Onofri@polytech.univ-mrs.fr

[(2)] IMECH, Bulgarian Academy of Sciences, 1113 Sofia (Bulgaria)

ABSTRACT

We propose to use *3-coherent* and coplanar laser beams to form a laser Doppler probe volume. Under such condition the probe volume exhibits 2-fringes patterns parallel to the optical axis *z* with a cosine amplitude modulation, see Figure 1. The Fourier transform of a Doppler signal produced by a small particle crossing this probe volume exhibits two Doppler frequency peaks. From the two frequencies, two estimations of the particle velocity component perpendicular to the fringes pattern are obtained. In addition, the amplitude ratio of the two frequency peaks is a direct measurement of the particle position along the *z-axis*. When considering a Phase Doppler system, two phase-shifts can be obtained at the same time by the proposed technique. This allows to extend the phase-shift measurement range from $[0,2p] \rightarrow [0,4p]$ and then, to extend by a factor of two the measurement size range or the size resolution.

In this paper, the principle of the proposed technique is investigated both theoretically and numerically. Rigorous numerical results based on Generalized Lorenz-Mie Theory (Gouesbet et al., 1988) are provided, demonstrating the advantages and limits of this technique.

As a typical numerical result, the spatial resolution of this technique is expected to be of $\pm 3\mu m$ for a measurement distance range of $\approx 100\mu m$; given a half-beam angle of $a = 2.28°$, Doppler signals with *SNR=10 dB* and for particles of a diameter bellow $\approx 1.6\mu m$. The measurement distance range can be easily controlled by adjusting the value of the half-beam angle.

This technique is though to be well adapted for micro-channel flows or boundary layers studies for which the determination of the particle position along the optical axis is important.

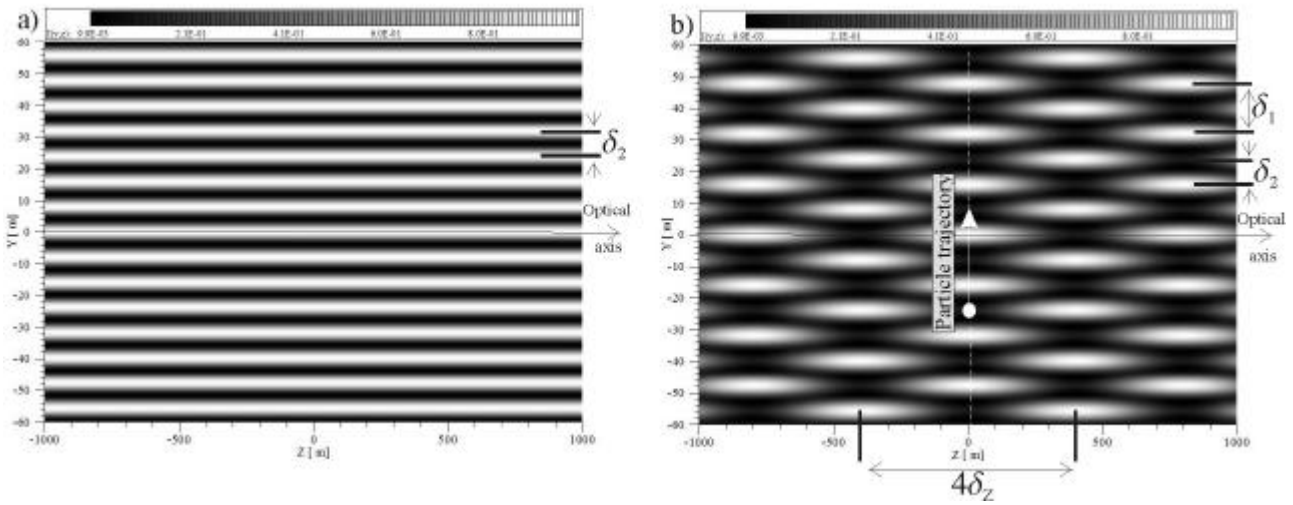

Fig. 1. Isolevels maps of the normalized intensity distribution calculated for the plane waves case.

a) *2-coherent* beams (+1,-1)

b) 3-*coherent* beams (+1,0,-1)

1. INTRODUCTION

The Laser Doppler Velocimetry (LDV) technique is one of the standard methods for spatial and time-resolved velocity measurements in fluids or multiphase flows. Nevertheless, the spatial resolution of this technique is not sufficient for some applications and it gives no information about the particle trajectory in the probe volume. For instance, this last point may be critical for boundary layer or micro-channel flow studies. Clearly, the main limiting parameter in the spatial resolution of this technique is the probe volume length. In the LDV principle, the probe volume is formed by the crossing of two coherent laser beams at their waist. The size of the nominal probe volume at $1/e^2$ is roughly ellipsoid with a diameter of $D_x \approx D_y \approx 2w_0/\cos\alpha$ and a length of $D_z \approx 2w_0/\sin\alpha$ (e.g. Durst et al., 1981), where α is the half-beam angle and $2w_0$ the laser beam waist at the probe volume centre. For $\alpha = 2.28°$ and $2w_0 = 200\mu m$, the optical probe volume length is as large as $D_z \approx 5mm$. To reduce the "measurement" probe volume length one classical solution is to use a collection optics with a sharp spatial filter (usually a slit). Depending on the magnification M of this optics, the slit width L and the mean collection angle θ, the measurement probe volume length is reduced to a slice of the initially ellipsoid probe volume of width $ML/\sin\theta$ ($\approx 150\mu m$ for $M = 3$, $L = 100\mu m$ and $\theta = 30°$).
More recently, Buettner and Czarske (2001) have proposed to use low coherence laser beams to reduce the nominal probe volume length. Despite the interest to this solution, as well as the one using a spatial filter, both of them do not provide any information about the particle trajectory in the probe volume.

The Phase Doppler (PD) technique is a direct extension of the LDV technique (e.g. Durst et al., 1975, Bachalo et al., 1984, Bauckhage et al., 1988). It allows performing simultaneous measurement of the velocity and the size of a particle crossing the probe volume. For classical PD systems the particle must be spherical, homogeneous and with a known refractive index, although solutions have been proposed to measure cylindrical (Mignon et al. 1996, Schaub et al. 1998, Onofri et al., 2003), inhomogeneous particles (Onofri et al. 1996a, 1999, 2000 and 2002, Manasse et al. 1994, Naqwi 1996, Göbel et al., 1997) or to determine on-line the particle refractive index (Naqwi et al., 1991, Onofri et al. 1996b and 1996c]. For the same reasons than for LDV, the excessive probe volume length is also a limiting point of this technique. Nevertheless, it causes additional problems as the size measurement requires being in the remote sensor condition and because the spatial filtering can induce erroneous measurements as discussed by Xu and Tropea (1994). One other well known limit of this technique is the 2π undetermination of the measured phase and then, the requirement to use more than two detectors to extend the size dynamic range or the size resolution (e.g. Albrecht et al., 2003).

In the present work we introduce the principle of a simple solution which could be helpful to determine the particle position along the optical axis in LDV and PD systems and also, to extend the size dynamic range or resolution of PD systems.

2. PRINCIPLE

We propose to use 3-coherent and coplanar laser beams to form the LDV or PD probe volume, see Figure 2. Classically, this probe volume can be produced by focusing the beam output from a coherent and linearly polarized laser onto a rotating transmission diffraction gratings (or a Bragg's cell, e.g. Durst et al, 1981). The particularity here is that we use the three main diffracted beams of order *-1, 0* and *1* to form the probe volume instead of two beams of order *+1, -1*. When the diffraction gratings is rotating, the beams ± 1 are frequency shifted by the quantity $\pm n_s$ from the laser beam frequency n while the beam *0* has no frequency shift. By collimating and focusing these three beams we produce the required probe volume.

As a first step, let us consider the incident beams as harmonic plane waves. In this case, the total electrical field in the probe volume reads:

$$E_T(y,z,t) = E_1 e^{j[\mathbf{k}_1.\mathbf{r}-2p(n+n_s)t]} + E_{-1} e^{j[\mathbf{k}_{-1}.\mathbf{r}-2p(n-n_s)t]} + E_0 e^{j[\mathbf{k}_0.\mathbf{r}-2pnt]} \quad (1)$$

With the help of the Poynting vector we can calculate the nominal intensity distribution in the *(y,z)* plane:

$$I(y,z,t) = \frac{k}{2\mu_0 w}\mathrm{Re}\left\{E_T E_T^*\right\} \quad (2)$$

It immediately follows that

$$I(y,z,t) \propto E_1^2 + E_{-1}^2 + E_0^2 + 2\mathrm{Re}\left\{E_1 E_{-1} e^{j[(\mathbf{k}_1-\mathbf{k}_{-1}).\mathbf{r}-4pn_s t]} + E_1 E_0 e^{j[(\mathbf{k}_1-\mathbf{k}_0).\mathbf{r}-2pn_s t]} + E_{-1}E_0 e^{j[(\mathbf{k}_0-\mathbf{k}_1).\mathbf{r}+2pn_s t]}\right\} \quad (3)$$

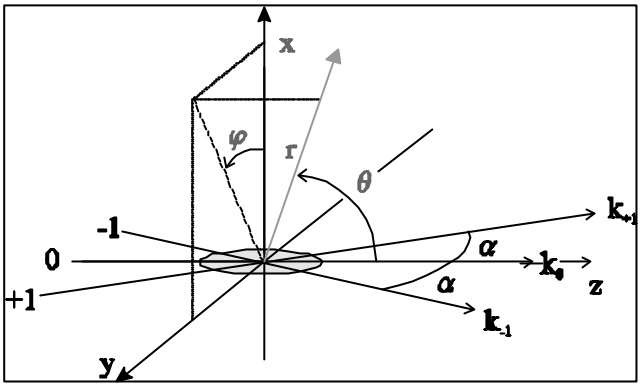

Fig. 2. Geometry of the intensity distribution and of the scattering models

After some calculations, we found that the intensity distribution takes the following form (with $E_{-1} = E_{+1}, E_0 \in \mathbb{R}$):

$$I(y,z,t) = 2E_1^2 \left\{1+\cos\left[4p\,\frac{\sin a}{l}\,y - 4pn_s t\right]\right\} + \left\{1+4E_1E_0\cos\left[2p\,\frac{\sin a}{l}\,y - 2pn_s t\right]\cos\left[\frac{2p}{l}(1-\cos a)\right]\right\} \quad (4)$$

To clarify the previous expressions, we introduce the following parameters:

$$d_1 = \frac{l}{\sin a} \quad (5)$$

$$d_2 = \frac{l}{2\sin a} \quad (6)$$

$$b = k(\cos a - 1) \quad (7)$$

Finally, the intensity distribution in the *(y,z)*-plane can be reformulated as follows:

$$I(y,z,t) = 2E_1^2 \left\{1+\cos\left[4p\,\frac{y}{d_2} - 4pn_s t\right]\right\} + \left\{1+4E_1E_0\cos\left[2p\,\frac{y}{d_1} - 2pn_s t\right]\cos[b\,z]\right\} \quad (8)$$

From the previous equation we can infer some important features of the intensity distribution in the probe volume :

- It exhibits two fringes pattern parallel to the *y-axis*. The first one has a fringes spacing equal to d_1 and the second one, a fringes spacing equal to d_2, with $d_1 = 2d_2$.
- The fringes pattern with fringes spacing d_2 corresponds to the usual one observed in a LDV system when only the beam pair $(-1,+1)$ interferes, see Figure 1 a). These fringes are "infinite" regarding to the *z-axis*.
- The fringes pattern with fringes spacing d_1 is "superimposed" to the first one, being produced by the beam pairs $(-1,0)$ and $(0,+1)$. In the small angle approximation ($a \approx 0°$, $\sin a \approx a$) we can consider that it is produced by a single pair of beams with crossing angle equal to $a/2$. The fringes are still parallel to the *y-axis* but they are modulated along the *z-axis* by a cosine function of period equal to $d_z = 2p/b$, see Figure 1 b).
- In the simple case where $E_0 = E_1 = E_{-1} = 1$, we find that the amplitude ratio of both fringes patterns varies in the limit of: $Min\{I(d_1,z,t)/I(d_2,z,t)\} = 1/9$ and $Max\{I(d_1,z,t)/I(d_2,z,t)\} = 9$.
- The two fringes patterns are also modulated in time, by the frequency $2n_s$ for the fringes pattern with spacing d_2 and n_s for the fringes pattern with spacing d_1.

We now consider a small particle with diameter $D \ll d_2$ moving in the probe volume along the *y-axis*, its trajectory is defined by: $\{y(t) = V_y t,\ z = 0\}$, see Figure 1b). In a first approximation, the light intensity scattered by this particle $I_S(y,z,t)$ is considered to be simply proportional to the intensity distribution in the probe volume (see the next Section): $I_S(y,z,t) \propto I(y,z,t)$. By assuming $E_1 = E_{-1} = E_0 = E$ and

$$n_1 = \frac{V_y}{d_1} - n_s \tag{9}$$

$$n_2 = \frac{V_y}{d_2} - 2n_s \tag{10}$$

the equation of a Doppler signal produced by the particle when it crosses the 3-coherent beams probe volume is:

$$I_S(y,z,t) \propto 2E^2\left\{\frac{3}{2} + \cos(2pn_2t) + 2\cos(2pn_1t)\cos b\,z\right\} \tag{11}$$

We now consider that the probe volume intensity distribution $I(y,z,t)$ along the *y-axis* is Gaussian: $E^2(y) = E^2(0)\exp\left[-2(y/w_0)^2\right]$. In fact, this allows taking into account a more realistic intensity distribution for the probe volume but we still neglect the laser beams phase distribution. Thus the amplitude of the Fourier transform $\left|S(n \geq 0)\right|$ of the Doppler signal $I_S(y,z,t)$ reads:

$$\left|S(n \geq 0)\right| = 3G(n)d(0) + G(n-n_1)d(n-n_1) + 2G(n-n_2)d(n-n_2)\left|\cos b\,z\right| \tag{12}$$

where $d(n)$ stands for the Dirac distribution and $\left|G(n)\right|$ for the Fourier transform of the temporal intensity profile $E^2(V_y t)$:

$$\left|G(n)\right| = \left|E^2(0)\sqrt{\frac{p}{2}}\frac{w_0}{V_y}\exp\left[-\frac{1}{2}\left(\frac{p\,w_0 n}{V_y}\right)^2\right]\right| \tag{13}$$

Here $\left|S(n \geq 0)\right|$ presents two peaks for $n \neq 0$: the lower frequency peak is centred on the "Doppler frequency" n_1, with an amplitude independent on the particle position along the *z-axis*; the higher frequency peak is centred on the Doppler frequency n_2 and its maximum amplitude depends on the particle position along the *z-axis*. The width of both peaks is controlled by the function $\left|G(n)\right|$. Classically, this width decreases with the particle transit time in the probe volume: $\propto w_0/V_y$.

If we measure the maximum amplitude of both peaks we can calculate a ratio which varies in the limits of $0 \leq R_n(z) \leq 2$:

$$R_n(z) = \frac{Max\{S(n_2)\}}{Max\{S(n_1)\}} = 2\left|\cos b\,z\right| \tag{14}$$

The principle of the proposed technique is then to deduce the particle position along the *z-axis* by inverting the previous equation:

$$z = \frac{1}{b}\left\{\cos^{-1}\left(\frac{1}{2}R_n(z)\right) \pm np\right\} \tag{15}$$

This position is determined modulo the distance $z = \pm np/b$, where *n* is a natural integer.

The particle velocity components along the *y-axis* can be determined in two ways:

$$V_y = (n_2 + 2n_s)d_2 \;\equiv\; (n_1 + n_s)d_1 \tag{16}$$

Theses frequencies correspond, in a first approximation, to probe volumes with half-beam angles equal to $a/2$ and a. Thus, when considering a Phase Doppler system, from the analysis of the phase of $S(n \geq 0)$ one can extract two phase-shift with a sensitivity to the particle diameter in a ratio of 1:2 (see next Section).

3 GAUSSIAN BEAMS AND RIGOUROUS SCATTERING MODEL

The previous model was helpful to obtain simple analytical expressions and then, to introduce the principle of the proposed technique. In the following, we develop a model which describes rigorously the laser beams and the scattering properties of the particle crossing the probe volume. To do so, we use the results of the Generalized Lorenz-Mie Theory (GLMT) for spheres: homogeneous (Gouesbet et al., 1988, 1994) or multilayered (Onofri et al., 1995). In the framework of

this theory, the electrical field scattered in the far field $(kr >> l)$ by a particle, arbitrary located in an arbitrary shaped beam, can be decomposed into two perpendicular components E_q and E_j :

$$\begin{aligned} E_q &= \frac{iE}{kr}\exp\left[-i(kr-2pnt)\right]S_2 \\ E_j &= \frac{-E}{kr}\exp\left[-i(kr-2pnt)\right]S_1 \end{aligned} \tag{17}$$

In Eq. (17) S_1 and S_2 are the complex scattering functions. They account for both the particle and incident beam properties. As usually with the Lorenz-Mie's theory (e.g. Bohren and Huffman, 1983) these functions take the form of infinite series

$$\begin{aligned} S_1 &= \sum_{n=1}^{\infty}\sum_{m=-n}^{+n}\frac{2n+1}{n(n+1)}\left[ma_n g_{n,TM}^m p_n^{|m|}(\cos q)+ib_n g_{n,TE}^m t_n^{|m|}(\cos q)\right]\exp[imj] \\ S_2 &= \sum_{n=1}^{\infty}\sum_{m=-n}^{+n}\frac{2n+1}{n(n+1)}\left[a_n g_{n,TM}^m t_n^{|m|}(\cos q)+imb_n g_{n,TE}^m p_n^{|m|}(\cos q)\right]\exp[imj] \end{aligned} \tag{18}$$

where m is the particle relative refractive index, a_n and b_n are the external scattering coefficients which depend on the particle properties (shape and refractive index), $t_n^{|m|}(\cos q)$, $p_n^{|m|}(\cos q)$ are generalized Legendre functions. The so-colled "beam shape coefficients" $g_{n,TM}^m$, $g_{n,TE}^m$ describe all the properties of the incident beam (intensity and phase distribution). For more details about GLMT the reader is referred to Gouesbet et al. (1998).

For a LDV or a PD system operating in a planar configuration (Aizu et al., 1994) with parallel polarisation (i.e. the collection optics and the incident electrical field vectors are in the *yz-plane*) the total electrical field scattered by the particle reduces to:

$$\mathbf{E}_T(\mathbf{r},q,p/2,t)=\left[E_{+1q}(q+a)+E_{-1q}(q-a)+E_{0q}(q)\right]\mathbf{e}_q \tag{19}$$

and for the total Poynting vector in the direction of the collection optics:

$$\left|\mathrm{S}(\mathbf{r},q,p/2,t)\right|=\frac{k}{2p\bar{n}\mu_0}\left[\left|E_{+1q}\right|^2+\left|E_{-1q}\right|^2+\left|E_{0q}\right|^2+2\mathrm{Re}\left\{E_{+1q}E_{-1q}^*+E_{+1q}E_{0q}^*+E_{-1q}E_{0q}^*\right\}\right] \tag{20}$$

The light intensity scattered by the particle and collected by the optics (with aperture solid angle Ω) reads :

$$I_S(\mathbf{r},t)=\int_{\Omega}\left|\mathrm{S}(\mathbf{r},q,p/2,t)\right|d\Omega \tag{21}$$

The previous expression allows for numerical calculation of the scattered intensity for various positions (see Figure 3) and trajectories (see Figures 4-10) of the particle in the probe volume. By introducing the classical integral quantities which characterize a Doppler signal: the pedestal *P*, the signal visibility *V* and the phase-shift **Φ**, Eq. (21) can be expressed in terms of both fringes patterns (see for more details Onofri et al., 2003):

$$\begin{aligned} P_1 &= \frac{k}{2p\bar{n}\mu_0}\left\langle\frac{1}{2}\left|E_{-1q}\right|^2+\frac{1}{2}\left|E_{+1q}\right|^2+\left|E_{0q}\right|^2\right\rangle_\Omega & P_2 &= \frac{k}{2p\bar{n}\mu_0}\left\langle\frac{1}{2}\left|E_{-1q}\right|^2+\frac{1}{2}\left|E_{+1q}\right|^2\right\rangle_\Omega \\ \langle H_1\rangle_\Omega &= \left\langle E_{+1q}E_{0q}^*+E_{-1q}E_{0q}^*\right\rangle_\Omega & \langle H_2\rangle_\Omega &= \left\langle E_{+1q}E_{-1q}^*\right\rangle_\Omega \\ V_1 &= 2\left|\langle H_1\rangle_\Omega\right|/P_1 & V_2 &= 2\left|\langle H_2\rangle_\Omega\right|/P_2 \\ \Phi_1 &= \tan^{-1}\left[-\mathrm{Im}\left(\langle H_1\rangle_\Omega\right)/\mathrm{Re}\left(\langle H_1\rangle_\Omega\right)\right] & \Phi_2 &= \tan^{-1}\left[-\mathrm{Im}\left(\langle H_2\rangle_\Omega\right)/\mathrm{Re}\left(\langle H_2\rangle_\Omega\right)\right] \end{aligned} \tag{22}$$

That is we get the following equation for a 3-coherent beams Doppler signal :

$$I(\mathbf{r},t)=P_1\left[1+V_1\cos(2pn_1t+f_1)\right]+P_2\left[1+V_2\cos(2pn_2t+f_2)\right] \tag{23}$$

The phase-shift f_2 is associated to the classical single beam pair (-1,+1) and the half-beam angle of a. The phase-shift f_1 is associated to the double beam pair (-1,0)+ (0,+1) with an expected "equivalent" half-beam angle of $a/2$. That is,

for a classical optical configuration, the phase-shift f_2 is expected to be two times more sensitive in respect to the particle diameter (or refractive index) than f_1.

3. NUMERICAL RESULTS AND DISCUSSION

In the following we do not present any results about the velocity as the resolution of the proposed technique, onto this parameter, is the same than for classical LDV.

3.1 Measurement of the particle position along the optical-axis, z-axis

Plane-wave case

Figure 1 presents the intensity distribution calculated from Eq. (8) for $a = 2.2790534°$, $l = 0.6328\mu m$ and $E_{+1} = E_{-1} = E_0 = 1$. These isolevels maps have been normalized by the maximum value.
In case of 2-coherent laser beams, the fringes are of constant amplitude regarding to the *z-axis* and are equally spaced along the *y-axis* with $d_2 \approx 7.96\mu m$, see Figure 1 a). In the case of 3-coherent beams a second modulation frequency appears along the *y-axis* with periodicity $d_1 \approx 15.91\mu m$, see Figure 1 b). The fringes amplitude modulation along the *z-axis* is well pronounced with periodicity equal to $4d_Z \approx 800\mu m$.

Gaussian beams

Figure 3 presents the isolevel map of the scattered intensity calculated with Eq. (21) for Gaussian beams ($2w_0 = 200\mu m$), the parallel polarisation ($j = p/2$), a collection angle of $q = 180°$ and a water droplet *(m=1.332, D=0.1µm)*. Figure 3 presents the results for a) 2-coherent beams and b) 3-coherent beams.

Figure 4 presents the Doppler signals that are produced by this water droplet when it crosses the probe volume with a trajectory parallel to the *y-axis* and for *z=0, 0.675*d_Z, d_Z, *2*d_Z and *15*d_Z. These signals have been simulated for the optical, particle and sampling parameters summarized in Table 1, and afterward, analyzed with a classical Fast Fourier Transform algorithm. The Doppler signals or "bursts" exhibit a double modulation frequency. In the corresponding Fourier spectra, the two frequency peaks are centred on the expected Doppler frequencies: $n_1 = V_y / d_1 - n_s \approx 3.61MHz$ and $n_2 = V_y / d_2 - 2n_s \approx 7.23MHz$. The amplitude ratio of both peaks depends clearly on the value of *z* with $R_n(z)$*=2.00, 0.99, 0.09, 2.07, 0.48* and *7.35* respectively to the aforementioned positions along *z*.

Half-beam angle, a [deg]	2.28	Particle diameter, D [µm]	0.1
Wavelength, l [µm]	0.6328	Particle refractive index, m [-]	1.332
Laser beam waist diameter, $2w_0$ [µm]	200	Particle nominal velocity, V_y [m/s]	22
Beams frequency shift, n_s [MHz]	5	Doppler signals sampling rate, [MHz]	50
Polarisation	□	Doppler signals length, $4w_0$ [µm]	400
Collection or scattering angle, q [deg]	180	Signal to Noise ratio, *SNR* [dB]	∞

Table 1: Optical, particle and sampling parameters used for the simulations

Figure 5 presents the evolution of the amplitude ratio $R_n(z)$ versus the offset of the particle trajectory along the optical axis *z*, for various laser beams waist diameters and for the parameters given in Table 1. For plane waves ($2w_0 \to \infty$) the evolution of $R_n(z)$ is the same as the one predicted by the intensity distribution model introduced in Section 2. It is periodic of period $2d_Z = 400\mu m$ and, as predicted in Section 2, $R_n(z)$ evolves from $\approx 1/9$ up to ≈ 2.0. These last remarks confirm our hypothesis that for small particles $D \ll d_2$ the scattered intensity and the intensity distribution in the probe volume are directly proportional.

In the case of Gaussian beams, the more the laser beams are focused the more the discrepancy with the plane wave model increases (i.e. $R_n(z)$ exceeds rapidly the maximum value predicted by Eq. (14)). This effect may be attributed to the curvature of the wave fronts and can be taken into account numerically or analytically with Eq. (24).

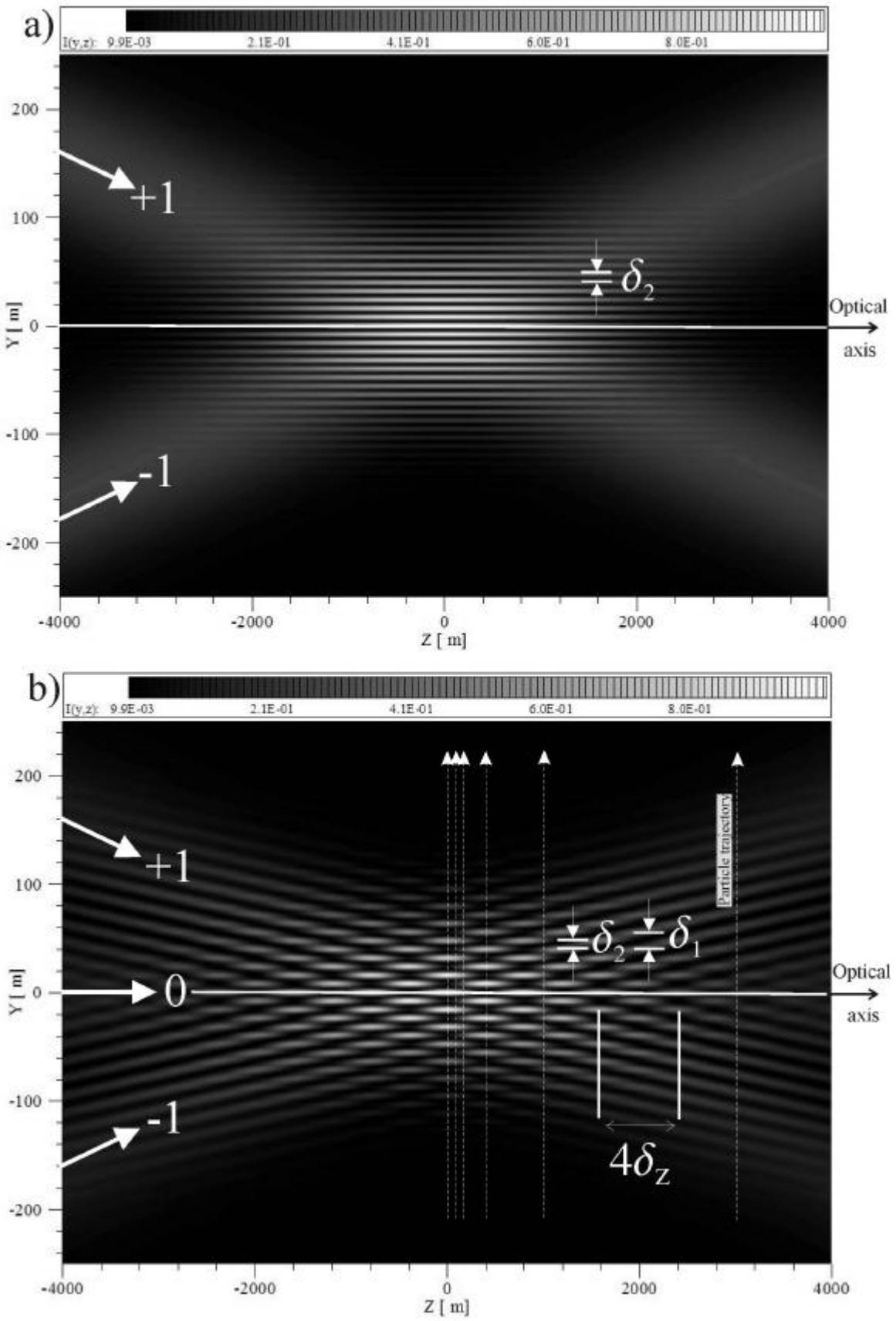

Fig.3. Isolevels maps of the normalized scattered intensity by D=0.1µm water droplet moving in the probe volume formed by:

a) 2-coherent Gaussian beams (+1,-1) with $2w_0$=200 µm

b) 3-coherent Gaussian beams (+1,0,-1) with $2w_0$=200 µm

Effects of the signal to noise ratio

Experimental LDV or PD signals are usually noisy. Figure 6, presents simulated Doppler signals with different level of Signal to Noise Ratio (*SNR*). The noise added is a white noise of known power with *SNR=40, 20, 10* and *5 dB*.
Figure 7 presents the corresponding evolution of $R_n(z)$. The error bars have been obtained statistically by simulating 500 particle trajectories for each value of *z*.
In contrary to the error bars, the mean evolution of $R_n(z)$ remains unchanged when increasing *SNR*.

We have simulated the evolution of $R_n(z)$ for various level of the *SNR* and for three cases: $E_0 = E_1/2$, $E_0 = E_1$ and $E_0 = 2E_1$. The results have shown that by increasing the amplitude of beam *0* we increase the amplitude modulation depth of $R_n(z)$. Unfortunately, in this way we also increase the sensitivity of $R_n(z)$ to the noise level so that, changing the relative amplitude of the incident beams does not improve the resolution on z_m.

Inversion of the amplitude ratio R_n(z)

To simulate experimental measurements of the offset of position of the particle along optical axis: z_m, we have inverted the results presented in Figure 7 by using Eq. (15), see Figure 8. The resolution on *z* is rather poor for positions where the cosine term in Eq. (14) is maximum (i.e. $z \approx \pm n2d_Z$). On the contrary the resolution increases significantly for positions where $z \approx \pm(2n+1)d_Z$. Note that there is an indetermination on z_m due to the periodicity of $R_n(z)$.
Following the last remarks, if we restrict the measurement position range to $z \in [0.45d_Z, 0.95d_Z]$ there is no more indetermination on z_m and we can improve significantly the resolution on z_m. In the present case, this positions range has a width *100 µm* for $z \in [90\mu m, 190\mu m]$.

For plane waves the evolution of $R_n(z)$ is given by Equation (15) with a very good approximation. Nevertheless, as shown in Figure 5 for focused beams, the laser beams divergence has some influence on the evolution of $R_n(z)$. This influence can be taken into account numerically. But, for $0 \le z \le d_Z$, we can also use the following corrected form for $R_n(z)$:

$$R_n(z) = b_1 \cos^{b_3}(b_2 z) \tag{24}$$

where the constants b_1, b_2, b_3 are deduced from the fitting of the theoretical evolution of $R_n(z)$, see Figure 10.

From the previous equation, the particle position along the optical axis can be determined with

$$z_m = \frac{1}{b_2}\cos^{-1}\left(\frac{R_n(z)}{b_1}\right)^{1/b_3} \tag{25}$$

Figure 10 presents the inverted position z_m versus the nominal position *z*, for a *SNR=10 dB* (see Figure 6) and 3 half-beam angles: $a = 1.24°, 2.28$ and $2.56°$. For each angle we can estimate both the average resolution of the proposed technique: $s_{Z_m} \approx \pm 12\mu m, \pm 3\mu m, \pm 1\mu m$ and the corresponding measurement range $\approx 400\mu m, 100\mu m, 25\mu m$.

3.2 Particle size influence and measurement

The principle of the proposed technique is somewhat based on the idea that by measuring the ratio of both fringes "visibility" we can deduce the particle position. This infers that the particle has no effect of this visibility. This is known to be true for particles much smaller than the fringes spacing (e.g. Durst et al., 1981). It is the reason why, to derive Eq. (14), we are restrict our approach to particles of $D \ll d_2$.
Figure 11 presents the evolution of $R_n(z)$ simulated with Eq. (21) for the parameters of Table 1 and several water droplet diameters. These diameters are expressed in fraction of the fringe spacing d_2.

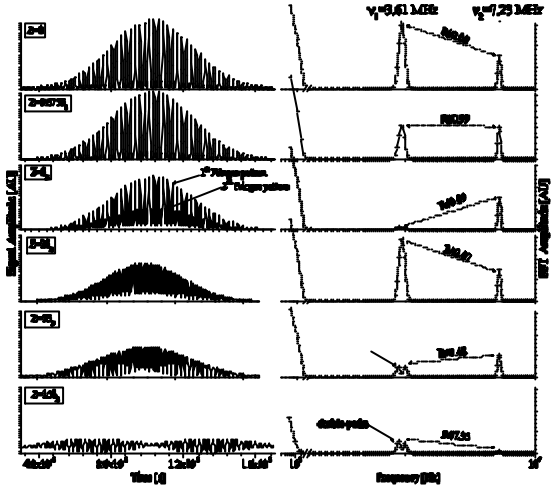

Fig.4. Doppler signals and their Fourier transforms at various values of z for a water droplet of D=0.1 µm whose trajectory is parallel to the y-axis.

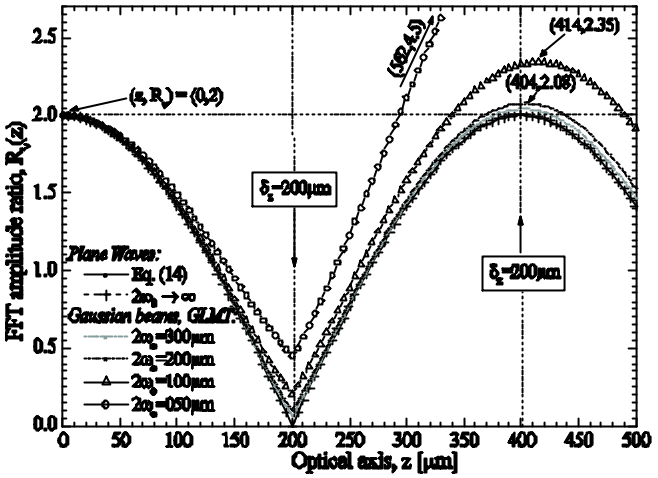

Fig.5. Evolution of the amplitude ratio of the two Doppler peaks for various beam waist diameters.

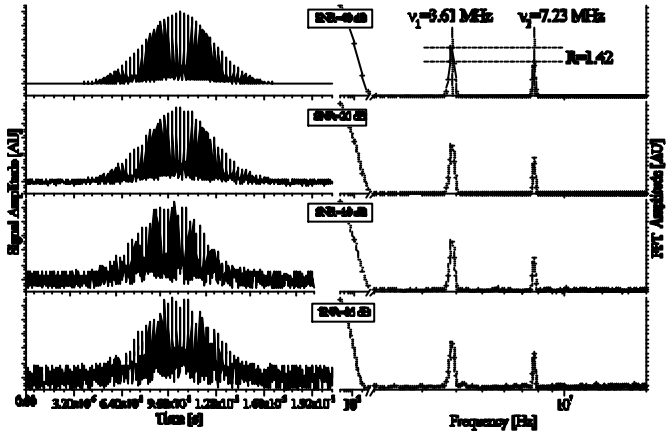

Fig.6. Doppler signals and their Fourier transforms for various levels of SNR (white noise added).

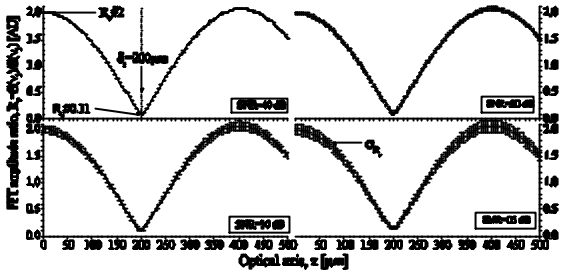

Fig.7. Evolution of R_n (z) for various levels of the SNR.

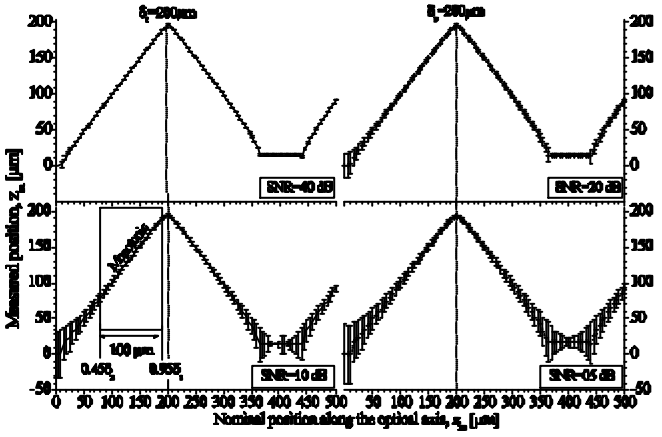

Fig. 8. Simulation of the measured position z_m versus the nominal particle position along the z-axis, with the level of SNR as a parameter (i.e. inversion of curves presented in Figure 7).

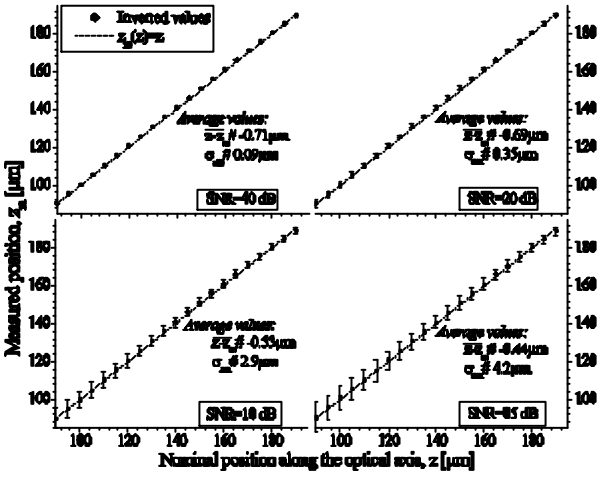

Fig. 9. Zooming on the first monotonic part of the measured positions z_m versus nominal positions, z.

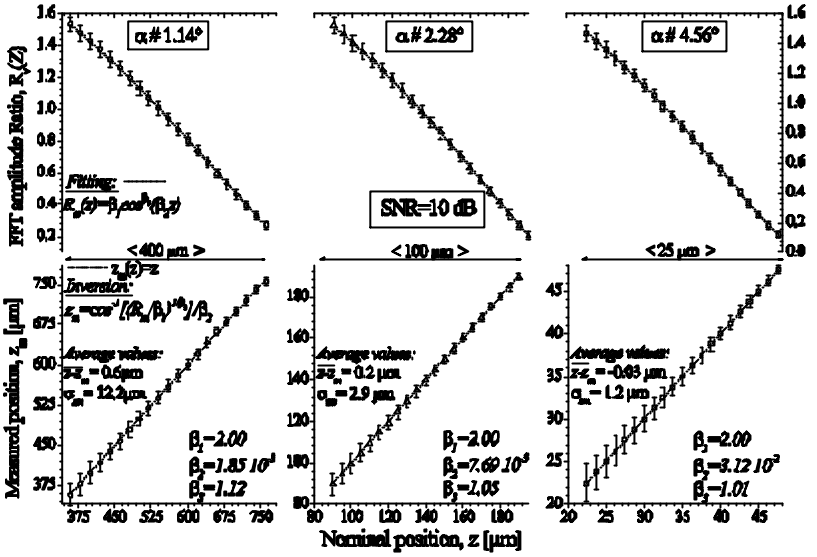

Fig.10. Evolution of $R_n(z)$ and z_m for a SNR=10 dB and three different values of the half-beam angle.

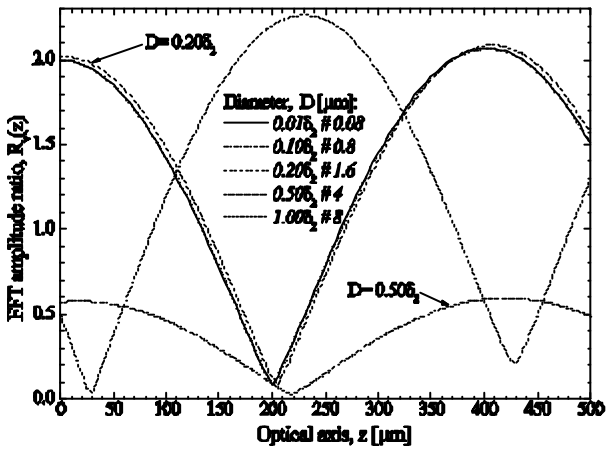

Fig.11. Influence on $R_n(z)$ of the particle diameter in respect to the minimum fringes spacing.

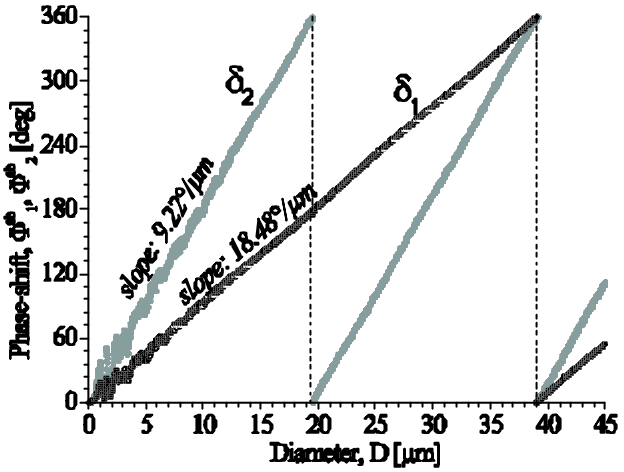

Fig.12. Phase-diameter relationships obtained simultaneously with a Phase Doppler system working with 3-coherent beams.

In Figure 11 it appears that for diameters up to $\approx 20\%$ of the fringes spacing d_2, the particle diameter D has no significant influence on the evolution of $R_n(z)$ as it is predicted by Eq. (14). For larger particles the evolution of $R_n(z)$ changes rapidly, in terms of amplitude modulation and phase (in respect to the probe volume centre). Its periodicity along the *z-axis* seems less sensitive to the particle diameter. This diameter dependence is one of the limits of the proposed technique. In fact, to get high resolution measurement on z_m the diameter of the particles must be $D \leq d_2/5$. For the optical parameters of Table 1, this means that for a measurable range of $100\mu m$ the diameter of the particles must smaller than $\approx 1.6\mu m$.

Nevertheless, thinking about the application of this technique to boundary layers and micro channel flows studies, this diameter dependence is not so critical as far as for such studies, the flow must be seeded by submicron particles.

As shown by Eq. (23) two phase-shifts can be extracted from the spectral analysis of Doppler signals produced by the proposed technique. Figure 12 presents the simulation of the two phase-diameter relationships obtained with a Phase-Doppler system using 3-coherent beams. The slopes of both phase-diameter relationships are in the ratio of $\approx 1:2$ as

expected theoretically. Note that the authors have recently developed a phase Doppler systems using 3-coherent beams to measure *on-line* the diameter (Onofri et al., 2003) and the tension (Onofri et al., 2004a) of reinforcement glass fibres during their forming process. Experimental results obtained with this system were found to be in excellent agreement with our theoretical predictions and with other experimental results (Onofri et al., 2004b).

6. CONCLUSION

In the present work, we have introduced a simple solution to allow determining the position of the particle along the optical axis by Laser Doppler Velocimetry and Phase Doppler techniques. For this purpose we use 3-*coherent* and coplanar laser beams to form the laser Doppler probe volume. The principle of the proposed technique is investigated both theoretically and numerically. Rigorous numerical results based on Generalized Lorenz-Mie Theory (Gouesbet et al., 1988) are provided, demonstrating the advantages and limits of this technique. As a typical numerical result the spatial resolution of this technique is of $\pm 3\mu m$ for a measurement distance range of $\approx 100\mu m$, given a half-beam angle of $a = 2.28°$, Doppler signals with $SNR = 10dB$ and for particles with a diameter bellow $\approx 1.6\mu m$. The measurement distance range can be easily controlled by adjusting the value of the half-beam angle.
In a future work, it will be demonstrated that this technique is well adapted for micro-channel flows or boundary layers studies for which the determination of the particle position along the optical axis is important.

ACKNOLEDGEMENTS

The authors are grateful to Saint-Gobain Recherche, the CNRS and the Bulgarian Academy of Science (PECO-NEI n°16939) for providing financial support for this work.

REFERENCES

Aizu Y., Domnick J., Durst F., Gréhan G., Onofri F., Qiu H.H., Sommerfeld M., Xu T.-H. and M. Ziema (1994), "A new Generation of Phase Doppler Instruments for Particle Velocity, Size and Concentration Measurements", Part. Part. Syst. Charact., 2, pp. 43-54

Albrecht H E, Damaschke N, Borys M and Tropea C (2003), "Laser Doppler and Phase Doppler Measurement Techniques", (Berlin: Springer)

Buettner L. and Czarske J. (2001), "A multimode-fibre laser-Doppler anemometer for highly spatially resolved velocity measurements using low-coherence light", Meas. Sci. Technol., 12, 1891–1903

Durst F. and Zaré M. (1975), "Laser Doppler measurements in two-phase flows", Proceedings of LDA-Symposium, Copenhagen, pp. 403-429

Durst F., Melling A. Whitelaw J.H. (1981), "Principles and Practice of Laser-Doppler Anemometry", Academic Press, London.

Bachalo W.D. and Houser M.J. (1984), "Phase/Doppler spray analyzer for simultaneous measurements of drop size and velocity distributions", Opt. Eng., 23, pp. 583-590

Bauckhage K. and Floegel H.H. and Fritsching U. and Hiller R. (1988), "The Phase Doppler difference method, a new laser Doppler technique for simultaneous size and velocity measurements", Part 2: Optical particle characteristics as a base for a new diagnostic technique, Part. Part. Syst. Charact., 5, pp. 66-71

Bohren C.F. and Huffman D.R. (1983), "Absorption and Scattering of Light by Small Particles", Wiley, New York.

Göbel G., Doicu A., Wriedt T., Bauckhage K. (1997) "Influence of surface roughness of conducting spheres on the response of a phase-Doppler anemometer". Part. Part. Syst. Charact., 14, pp. 283–289

Gouesbet G., Maheu B. and Gréhan G. (1988), "Light scattering from a sphere arbitrarily located in a Gaussian beam, using a Bromwich formulation", J.O.S.A. A. 9, pp. 1427-1443

Gouesbet G. and Lock J.A (1994), "Rigourous justification of the localized approximation to the beam shape coefficients in the generalized Lorenz-Mie theory. I/ Off-axis beams", J. Opt. Soc. Am. A, 11, pp. 2503-2515

Gouesbet G., Grehan G., Maheu B. and Ren K. F (1998), "Electromagnetic Scattering of Shaped Beams (Generalized Lorenz-Mie Theory)", unpublished book, LESP-CORIA, INSA de Rouen, Saint Etienne du Rouvray, France

Manasse U., Wriedt T., Bauchhage K. (1994), "Reconstruction of real size distributions hidden in PDA results obtained from droplets of Inhomogeneous liquids", Part. Part. Syst. Charat., 11, pp. 84-90

Mignon H., Gréhan G., Gouesbet G., Xu T-H. and Tropea C. (1996), "Measurement of cylindrical particles with phase Doppler anemometry", Appl. Opt., 35, pp. 5180-5190

Naqwi A., Durst F. and Liu X. (1991), "Two optical methods for simultaneous measurement of particle size, velocity, and refractive index", Appl. Opt., 30, pp.4949-4959

Naqwi A. (1996), "Sizing of Irregular Particles Using a Phase Doppler System", Part. Part. Syst. Charact., 8, pp. 343-349.

Onofri F., Gréhan G., Gouesbet G. (1995), "Electromagnetic scattering from a multilayered sphere located in an arbitrary beam", Appl. Opt., 30, pp. 7113-24.

Onofri F., Blondel D., Gréhan G., Gouesbet G. (1996a), "On the Optical Diagnosis and Sizing of Coated and Multilayered Particles with Phase Doppler Anemometry", Part. and Part. Syst. Charact., 13, pp. 104-111.

Onofri F., Girasole T., Gréhan G., Gouesbet G., Brenn G., Domnick J., Tropea C., Xu T-H. (1996b), "Phase-Doppler Anemometry with Dual Burst Technique for Measurement of Refractive Index and Absorption Coefficient Simultaneous with Size and Velocity", Part. and Part. Syst. Charact., 13, pp. 212-24.

Onofri F., Bultynck H. and Gréhan G. (1996c), « Mesures Corrélées Taille-Vitesse-Indice Par Anémométrie Phase Doppler : Application à l'étude des phénomènes de coalescence et mesure de la température de particules », in 5ème Congrèss Francophone de Vélocimétrie Laser, 25-27 Septembre, Rouen (France), paper E3

Onofri F., Bergounoux L., Firpo J-L., Mesguish-Ripault J. (1999), "Velocity, size and concentration measurements of optically inhomogeneous cylindrical and spherical particles", Appl. Opt., 38, pp. 4681-90.

Onofri F. (2000), « Etude numérique et expérimentale de la sensibilité de l'Anémométrie Phase Doppler à l'état de surface des particules détectées », 7ème Congrès Francophone de Vélocimétrie Laser, Marseille, pp. 335-342

Onofri F, Lenoble A and Radev S (2002), "Superimposed non interfering probes to extend the phase Doppler anemometry capabilities", Appl. Opt., 41, pp.3590-3600

Onofri F, Lenoble A, Radev S, Bultynck H, Guering P H and Marsault N (2003), "Interferometric sizing of single-axis birefringent glass fibers", Part. Part. Syst. Charact., 20, pp.171-182

Onofri F., Lenoble A., Radev S., Guering P-H (2004a), Optical measurement of the drawing tension of small glass fibres, Meas. Sc. Tech., under press.

Onofri F., Lenoble A., Bultynck B., Guéring P-H (2004b), "High-resolution laser diffractometry for the on-line sizing of small transparent fibres", Opt. Com., 234, pp. 183-191

Schaub S., Naqwi A. and Harding F.L. (1998) "Design of a phase/Doppler light-scattering system for measurement of small-diameter glass fibers during fibers glass manufacturing", Appl. Opt., 37, pp. 573-585

Xu T.-H., Tropea C. (1994) "Improving the Performance of Two-Component Phase Doppler Anemometers", Meas. Sci. Technol., 5, pp. 969-975